

On the Thermodynamic Geometry of Hot QCD

Stefano Bellucci^{a,*}, Vinod Chandra^{b,c,†} and Bhupendra Nath Tiwari^{a,‡}

^a *INFN-Laboratori Nazionali di Frascati, Via E. Fermi 40, 00044 Frascati, Italy.*

^b *Department of Physics, Indian Institute of Technology Kanpur, Kanpur- 208 016, India. and*

^c *Department of Theoretical Physics, Tata Institute of Fundamental Research, Homi Bhabha Road Mumbai-400005, India.*

We study the nature of the covariant thermodynamic geometry arising from the free energy of hot QCD. We systematically analyze the underlying equilibrium thermodynamic configurations of the free energy of 2- and 3-flavor hot QCD with or without including thermal fluctuations in the neighborhood of the QCD transition temperature. We show that there exists a well-defined thermodynamic geometric notion for the QCD thermodynamics. The geometry thus obtained has no singularity as an intrinsic Riemannian manifold. We further show that there is a close connection of this geometric approach with the existing studies of correlations and quark number susceptibilities.

Keywords: Thermodynamic Geometry, Hot QCD, Quasi-particles.

PACS: 12.38.-t; 05.70.Fh; 02.40.Ky; 12.40.Ee

I. INTRODUCTION

Motivated from string theory, D-brane physics and black hole thermodynamics, we focus on investigating the possibilities of covariant thermodynamic geometric study of hot QCD near the QCD transition temperature. In particular, we intend to study the thermodynamic geometry arising from the free energy for the 2- and 3-flavor finite temperature QCD. The main idea of the present paper is first to develop a geometric notion for QCD thermodynamics and then to relate it with the existing microscopic quantities already known from the physics of hot QCD [1, 2]. We further incorporate thermal fluctuations in the free energy [3] and thus study their contributions to the thermodynamic geometry.

Let us recall that the existence of the covariant geometric structure in equilibrium thermodynamics was introduced by Weinhold [4] through an inner product in the space of equilibrium thermodynamic macrostates defined by the minima of the internal energy function $U = U(\nu_i, v, s)$ as the Hessian function $h_{ij} = \partial_i \partial_j U$. Here, the reduced quantities $\{\nu_i, v, s\}$ may respectively be defined as the underlying chemical potentials μ_i , volume V and that of the entropy S scaled with temperature of the considered equilibrium configuration. In order to provide a physical scale and to restrict negative eigenvalues of the metric tensor, we require that the volume and other parameters be held fixed for the subsequent analysis of the QCD configurations.

Interestingly, the Riemannian geometric structure thus involved indicates certain physical significance ascribed to hot QCD. The associated inner product structure on the intrinsic space may either be formulated in the entropy representation, as a negative Hessian matrix of the entropy with respect to the extensive variables, or that of the energy representation, as the Hessian matrix of the

associated energy with respect to the intensive variables. Such geometric considerations have been studied earlier in the literature as the covariant thermodynamics whose application in the energy representation has first been considered by Weinhold [4]. On the other hand, the entropy representation has been considered in Ruppeiner's fluctuation theory [5, 6].

In this paper, we shall take the former picture and study the covariant thermodynamic geometric properties ascribed to hot QCD. The thermodynamic macrostates of an underlying equilibrium chemical potential space may in turn be described by the minima of the energy function $F = F(U, V, N)$. Explicitly, the thermodynamic metric tensor of an intrinsic Riemannian space spanned by the chemical potentials may be given as $g_{ij} = \partial_i \partial_j F(\mu_i, T, V, S)$ and turn out to be conformal to the Ruppeiner metric with the temperature as the conformal factor. The intrinsic metric as an inner product on the (hyper-)surface of chemical potentials is thus necessarily ensured to be symmetric, positive definite and satisfies the triangle inequality since the energy function has a minimum configuration in the equilibrium.

On other hand, the thermodynamic geometry of the equilibrium configurations thus described has extensively been applied to study the thermodynamics of a class of black hole configurations [7]. Recent studies of the thermodynamics of diverse black holes in the state-space geometric framework have elucidated interesting aspects of phase transitions and their relations associated with the extremal black hole solutions in the context of the moduli spaces of $N \geq 2$ supergravity compactifications [8]. It may be argued however that the connection of such geometric formulations to the fluctuation theory of black holes thermodynamics requires several modifications [9]. The geometric formulation involved has first been applied to $N \geq 2$ supergravity extremal black holes in $D = 4$ which arise as low energy effective field theories from compactification of Type II string theories on Calabi-Yau manifolds [10]. Since then, several authors have attempted to understand this connection [11, 12] both for supersymmetric as well as non-supersymmetric black

* bellucci@lnf.infn.it

† joshi.vinod@gmail.com, Current affiliation of the author is c

‡ tiwari@lnf.infn.it

holes and five dimensional rotating black rings. The geometric notions remain well-defined for the diverse cases of extremal and non-extremal black branes [7].

Here, we shall study the standard two dimensional thermodynamic geometry associated with the space of chemical potentials $\{\mu_1, \mu_2\}$ in the framework of quasi-particle theories of QCD. The application of the above geometric notions, as in any conventional thermodynamical systems, suggests that the space defined by the chemical potentials indicates the nature of the underlying statistical system. In particular, such geometric notions, like the covariant nature of the metric tensor and non-zero scalar curvature, shed light on the interactions present in the system. It is shown further that the associated conformally related thermodynamic scalar curvature defines the chemical correlation length of the system.

As a matter of fact, a few simple manipulations illustrate that the conformal thermodynamic curvature is inversely proportional to the singular part of the free energy associated with long range correlation(s) whose divergences consequently signify certain phase transition(s) at the critical point(s) of the QCD. It is worth to mention that the Ruppeiner formalism may further be applied to diverse condensed matter systems with two dimensional intrinsic Riemannian spaces, which has been found to be completely consistent with the scaling and hyper scaling relations involving certain critical phenomena and in turn reproduces the corresponding critical indices [5].

The purpose of the present paper is to investigate the relation between the covariant thermodynamic geometry and the quark-number susceptibility tensor, both of which have recently received considerable attention from the perspective of black hole physics and QCD thermodynamics. Thus, the goal here is to explore underlying microscopic arguments behind the notion of the covariant thermodynamic geometry arising from the free energy of certain QCD thermodynamic configurations. In general, it is however known in the context of quasi-particle models [1] that the quark number susceptibilities are defined as $\chi_{ij} \equiv \frac{\partial \mathcal{N}_i}{\partial \mu_j} = \frac{\partial^2 P}{\partial \mu_i \partial \mu_j} = \chi_{ji}$. Here i, j are flavor indices, \mathcal{N}_i is the quark number density, and P is the associated pressure of the QCD configurations.

In this framework, it has further been shown that lattice measurements of the off-diagonal susceptibility χ_{ud} determine the associated physical properties of the quark-gluon plasma. As reported in Ref. [2], these are shown to be consistent with Hard Thermal Loop (HTL) studies down to the temperature of order as low as that of $2.5T_C$, see also [13]. Blaizot, Iancu and Rebhan have in particular analytically computed the quark number susceptibilities for the quark gluon plasma at finite temperature within the self-consistent resummation of Hard Thermal/Dense Loop (HTL/HDL) [14]. Interestingly, these predictions at zero chemical potential were found to be consistent with the lattice results.

Note that all the diagonal and off-diagonal elements of χ_{ij} become equal at $\mu_i = 0$, and thus the quark number susceptibility tensor reduces to two different sectors, and

in particular, we have $\chi_{ij} \Big|_{\mu=0} \equiv \chi$ for $i = j$, and that of $\chi_{ij} \Big|_{\mu=0} \equiv \tilde{\chi}$ for $i \neq j$. In this paper, we have shown that the same remains true for the components of the covariant thermodynamic metric tensor which may further be regarded as the above quark number susceptibility tensor. In turn, this equivalence explains that the involved macroscopic/ microscopic duality relations, in our investigations of the 2 and 3-flavor QCD near transition temperature, turn out to be in a close connection with the AdS/CFT correspondence [15]. The present analysis indicates a sort of duality relationship between the macroscopic thermodynamic geometry and microscopic quark number susceptibility. The above formalism remains valid away from the limit of $\mu_i \neq 0$. We note further that the microscopic formalism is based on the evaluation of the diagonal susceptibility χ in a chosen resummation scheme, which directly follows from the expression of the fermion number density \mathcal{N} . From the viewpoints of microscopic theory, it is worth mentioning that the susceptibility tensor χ may be expressed in terms of the associated dressed fermion propagators as a function of the self-energies and fermions helicities [16].

On the other hand, the off-diagonal susceptibility tensors may be classified by the symmetry of the charge conjugation, or that of the C-parity. In particular, this in terms of chemical potentials means that a quark loop with two gluon external lines is necessarily even in the chemical potentials, while a quark loop with three gluon legs may also generate a linear term in the chemical potentials, which turns out to be symmetric in the color indices. We thus find an interesting match that the even derivative geometric quantities like the components of the metric tensor or the associated determinants and the thermodynamic scalar curvature as the fourth derivative invariant quantity turn out to be even in the chemical potentials. We envisage further that the components of thermodynamic metric tensor microscopically correspond to those of the susceptibility tensor and thus require two fermion loops connected by a set of gluon lines.

As the final exercise, we discuss the thermodynamic geometry of hot QCD including the thermal fluctuations over an equilibrium configuration of the chemical potentials. As it is well known, any thermodynamical system which may be considered as an ensemble has logarithmic and polynomial contributions to the free energy [3]. Moreover, such a connection have earlier been explored from the perspective of black hole physics, showing that the thermodynamic Ruppeiner geometry of the non-extremal rotating BTZ black holes, as well as that of the BTZ-Chern Simons black holes, get modified under the thermal fluctuations [17]. Subsequently, the thermodynamic geometry remains flat with and without the higher derivative contributions to the entropy.

In the context of QCD, what follows next that such geometric notions implicitly assume an equilibrium statistical basis defined in terms of an ensemble, and thus one may explore the role of thermal fluctuations in the free

energy and consequently on an associated intrinsic Riemannian geometry corresponding to the quasi-particle theories. For example, the canonical free energy corrected by the contributions coming from thermal fluctuations may be regarded as a closer approximation to that of the free energy in the corresponding ensemble. We here show that such considerations apply as well to the hot QCD ensembles, and the specific forms of the logarithmic and polynomial contributions can easily be calculated for a wide class of quasi-particles theories. It is to be noted that the applicability of this analysis presupposes that the underlying ensemble is thermodynamically stable, which requires a positive specific heat, or correspondingly that the Hessian matrix of the free energy function must be positive definite. The free energy function for any thermodynamical system incorporating such contributions [3] can easily be written as $F = F_0 + \ln(CT^2)$. In this article, we have shown that such logarithmic contributions to the free energy induces a set of bumps in the scalar curvature of the intrinsic thermodynamic space, spanned by the quark chemical potentials.

The paper is organized as follows. In the first section, we have presented the motivations to study the intrinsic Riemannian space obtained from the Gaussian fluctuations of the QCD free energy. In particular, we have outlined microscopic implications of the geometric QCD from the viewpoint of AdS/CFT correspondence. The remaining significance of the present analysis are summarized in the final section. In section 2, we have introduced very briefly the notion of thermodynamic geometry for the quasi-particles. In section 3, we obtain the 2- and 3-flavor QCD free energy and temperature near the T_C^0 , and express them as a function of the quark chemical potentials and thereby incorporate the thermal contributions into the free energy. In section 4, we analyze the thermodynamic geometry of two-flavor QCD in the framework of the quasi-particle theory with and without the logarithmic contributions.

In section 5, we focus our attention on the thermodynamic geometry of the 3-flavor QCD configurations. Explicitly, we investigate the nature of the thermodynamic geometry thus defined as an intrinsic Riemannian manifold obtained from the free energies with or without the contributions being considered in the section 4. We have explained that such a geometry obtained from the free energy of the quasi-particle theories results to be well-defined and pertains to an interacting statistical system. Finally, section 6 contains concluding issues and discussion of the thermodynamic geometry for both the 2-flavor and the 3-flavor hot QCD and the concerned microscopic implications arising from the underlying QCD, and thus it offers a physical explanation of finite chemical potential macroscopic/microscopic duality relations in a close connection with the AdS/CFT correspondence.

II. THERMODYNAMIC GEOMETRY

In this section, we present a brief review of the essential features of thermodynamic geometries from the perspective of the application to the hot QCD. In particular, we shall focus our attention on the geometric nature of the QCD thermodynamics in the neighborhood of QCD transition temperature, T_C with a finite number of quark chemical potentials introduced within the framework of quasi-particles theories.

Let us consider an intrinsic Riemannian geometric model whose covariant metric tensor may be defined as the Hessian matrix of the free energy with respect to an arbitrary finite number of chemical potentials carried by the quasi-particles in a given thermodynamic configuration at a fixed volume or any other parameters of the equilibrium QCD. In particular, let us define a representation $F(\mu_i, T)$ for given any free energy, chemical potentials, and temperature $\{F, \mu_i, T\}$ and then choose a particular temperature slice as an intersection of the line $T := T_C^{(0)}$ with the space spanned by the underlying chemical potentials $\{\mu_i, T\}$, that is to define the temperature as in Eq. 11. In this consideration, the free energy thus defined may further be shown to be only a function of the quark chemical potentials, which in fact we have indicated in general by Eqs. 12, 14. This method in general turns out to be an intrinsic Riemannian geometry, which is solely based on nothing other than the quark chemical potentials. This thus yields that the space spanned by the n chemical potentials of the theory under consideration exhibits a n -dimensional intrinsic Riemannian manifold M_n . The components of the covariant metric tensor, i.e. the so called thermodynamic geometry [5, 6, 12, 17] may be defined as

$$g_{ij} := \frac{\partial^2 F(\vec{x})}{\partial x^j \partial x^i}, \quad (1)$$

where the vector $\vec{x} = (\mu^i) \in M_n$. Explicitly for the case of two dimensional intrinsic geometry, the components of the thermodynamic metric tensor are

$$\begin{aligned} g_{\mu_1 \mu_1} &= \frac{\partial^2 F}{\partial \mu_1^2}, \\ g_{\mu_1 \mu_2} &= \frac{\partial^2 F}{\partial \mu_1 \partial \mu_2}, \\ g_{\mu_2 \mu_2} &= \frac{\partial^2 F}{\partial \mu_2^2}. \end{aligned} \quad (2)$$

Now we can calculate the Γ_{ijk} , R_{ijkl} , R_{ij} and R for above two dimensional thermodynamic geometry (M_2, g) and may easily see that the scalar curvature is given by

$$\begin{aligned} R &= -\frac{1}{2}(F_{\mu_1 \mu_1} F_{\mu_2 \mu_2} - F_{\mu_1 \mu_2}^2)^{-2} (F_{\mu_2 \mu_2} F_{\mu_1 \mu_1 \mu_1} F_{\mu_1 \mu_2 \mu_2} \\ &\quad + F_{\mu_1 \mu_2} F_{\mu_1 \mu_1 \mu_2} F_{\mu_1 \mu_2 \mu_2} + F_{\mu_1 \mu_1} F_{\mu_1 \mu_1 \mu_2} F_{\mu_2 \mu_2 \mu_2} \end{aligned}$$

$$\begin{aligned}
& -F_{\mu_1\mu_2}F_{\mu_1\mu_1\mu_1}F_{\mu_2\mu_2\mu_2} - F_{\mu_1\mu_1}F_{\mu_1\mu_2\mu_2}^2 \\
& -F_{\mu_2\mu_2}F_{\mu_1\mu_1\mu_2}^2.
\end{aligned} \tag{3}$$

Furthermore, the relation between this thermodynamic scalar curvature and the thermodynamic curvature tensor for such a two dimensional thermodynamic intrinsic geometry (see for details [7]) is given by

$$R = \frac{2}{\|g\|} R_{\mu_1\mu_2\mu_1\mu_2}, \tag{4}$$

which is quite usual for any intrinsic Riemannian surface $(M_2(R), g)$.

Note that such Riemannian structures defined by the metric tensor in a chosen representation are in fact closely related to classical thermodynamic fluctuation theory [6] and critical phenomena. The probability distribution of thermodynamic fluctuations in the equilibrium intrinsic space naturally characterizes the invariant interval of the corresponding thermodynamic geometry, which in the Gaussian approximation reads $\Omega(x) = A \exp[-\frac{1}{2}g_{ij}(x)dx^i \otimes dx^j]$, where the pre-factor A is the normalization constant of the Gaussian distribution. The associated inverse metric may easily be shown to be the second moment of the fluctuations or the pair correlation functions and thus may be given as $g^{ij} = \langle X^i | X^j \rangle$, where $\{X_i\}$'s are the intensive thermodynamic variables conjugated to $\{x^i\}$. Moreover, such Riemannian structures may further be expressed in terms of any suitable thermodynamic potential obtained by certain Legendre transform(s) which corresponds to general coordinate transformations on the equilibrium intrinsic manifold. Our geometric formulation thus tacitly involves a statistical basis in terms of a chosen ensemble, although the analysis has only been considered in the thermodynamic limit of QCD.

We wish to mention that the thermodynamic curvature corresponds to the nature of the correlation present in the statistical system. This in particular will imply that the scalar curvature for two component systems can be thought of as the square of the correlation length at some given QCD transition temperature $T_C(\mu_1, \mu_2)$ to be $R(\mu_1, \mu_2) \sim \xi^2$, where we may identify the $\xi(T_C)$ to be the correlation length of the thermodynamic system. In turn, it is not surprising that the geometric analysis based on a Gaussian approximation to the classical fluctuation theory precisely yields the correlation volume of QCD. This strongly suggests that even in the context of chemical reactions in any closed systems, non-zero scalar curvature might provide useful information regarding the possible interactions between various components of the QCD configuration.

Note further that the relation of a non-zero scalar curvature with an underlying interacting statistical system remains valid even for higher dimensional intrinsic manifolds and the connection of a divergent scalar curvature with phase transitions may accordingly be divulged from the Hessian matrix of the considered QCD free energy. It is worth to mention that our analysis takes an account of

the scales that are larger than the correlation length and considers that only few QCD microstates do not dominate the macroscopic quantities. In particular, we shall focus on the interpretation that the underlying QCD free energy includes contributions from a large number of microstates and thus our description of the geometric QCD thermodynamics. With this general introduction to the thermodynamic geometry defined as the Hessian function of the free energy, let us now proceed to investigate the free energy of hot QCD and its thermo-geometric structures. We now proceed to compute the QCD free energies in the required form and thereafter study the thermodynamic geometry of the quark theories arising from the free energy of hot QCD.

III. THE FREE ENERGY OF HOT QCD

To obtain the free energy as a function temperature and quark chemical potentials, we consider the quasi-particle model of hot QCD. We consider two cases in the present paper *viz.* the 2-flavor QCD with two distinct chemical potentials ($\mu \sim (\mu_1, \mu_2)$) and the 3-flavor QCD with two distinct chemical potentials (μ_1 corresponds to up and down quarks and μ_2 corresponds to strange quark). In order to obtain the expression for the free energy we consider the following equilibrium distribution functions for gluons and quarks:

$$\begin{aligned}
f_{eq}^g &= \frac{1}{(\exp(-\beta\epsilon_p) - 1)}, \\
f_{eq}^q &= \left\{ \frac{1}{(\exp(-\beta\epsilon_p - \beta\mu) + 1)} + \frac{1}{(\exp(-\beta\epsilon_p + \beta\mu) + 1)} \right\}.
\end{aligned} \tag{5}$$

To obtain the free energy one utilizes the well known thermodynamic relation,

$$F = -\frac{1}{\beta V} \left(\ln(Z_g) + \ln(Z_M) \right), \tag{6}$$

which is nothing but the negative of the pressure of hot QCD. Here Z_g and Z_M are the grand canonical partition functions corresponding to the pure gluonic part and matter sector respectively and have the following well known form in terms of the gluons and quark-antiquark distributions functions:

$$\begin{aligned}
\ln(Z_g) &= -\sum_p \ln(1 - \exp(1 - \exp(-\beta\epsilon_p))), \\
\ln(Z_M) &= \sum_p \left(\ln(1 + \exp(-\beta(\epsilon_p - \mu))) \right. \\
&\quad \left. + \ln(1 + \exp(-\beta(\epsilon_p + \mu))) \right).
\end{aligned} \tag{7}$$

We now turn our attention to compute the free energy in the small chemical potential limit ($\beta|\mu| \ll 1$). We

shall determine the free energy only up to quartic terms in $\beta\mu$. The expression thus obtained reads in compact notations as

$$F = T^4 \left(a_0 + c_1 \frac{\mu_1^2}{T^2} + c_2 \frac{\mu_2^2}{T^2} + c_4^1 \frac{\mu_1^4}{T^4} + c_4^2 \frac{\mu_2^4}{T^4} \right) + T^4 O(\mu^6/T^6). \quad (8)$$

We shall firstly consider the first three terms for our analysis which we denote as case (A) and the full expression will be denoted as case (B). We shall study these two cases systematically and thereby show that the geometric quantities remain intact at zero chemical potentials. On comparison of the free energy displayed in Eq.8 for 2- and 3-flavors with the temperature dependence of the corresponding pressure either in lattice QCD [18–20] or improved pQCD [21–24], one may conclude that the coefficients of the μ_1^2 and μ_2^2 should be negative in the corresponding pressure. We shall utilize this to fix the sign of the various terms in the Taylor expansion of the free energy as a function of the chemical potentials (μ_1 and μ_2). The various coefficients in Eq.8 for 2 and 3-flavour QCD are as follows:

For 2-flavor QCD,

$$a_0 = -\frac{8\pi^2}{45} \left(1 + \frac{42}{32} \right), c_1 = c_2 = 1/2, c_4^1 \equiv c_4^2 = -\frac{1}{4\pi^2} \quad (9)$$

For 3-flavour case, the above coefficient reads

$$a_0 = -\frac{8\pi^2}{45} \left(1 + \frac{63}{32} \right), c_1 = 1, c_2 = 1/2, c_4^1 = -\frac{1}{2\pi^2}, \quad (10)$$

$$c_4^2 = -\frac{1}{4\pi^2}.$$

Note that, all the above coefficients are dimensionless. Let us now turn our attention to analyze the free energy of hot QCD near T_C and trade off the T_C dependence in favour of quark chemical potentials resulting the following the relation [25]

$$\frac{T_c(\mu)}{T_c^0} = 1 + \sum_{i=1}^2 \tilde{a}_i \frac{\mu_i^2}{(T_c^0)^2}. \quad (11)$$

where $\tilde{a}_1 = \tilde{a}_2 = -0.07$ for the 2-flavor case and $\tilde{a}_1 = \tilde{a}_2 = -0.114$ for 3-flavor QCD. For the purpose of the subsequent analysis we choose $T_c^0 = 0.203$ GeV for $N_f = 2$ QCD and $T_c^0 = 0.197$ GeV in 3-flavor QCD [26]. After substituting for the transition temperature T_C , as the function of quark chemical potentials in the free energy, we thus obtain the following polynomial form for the free energy:

$$F(\mu_1, \mu_2) := a_0(b + a_1\mu_1^2 + a_2\mu_2^2)^4 + (b + a_1\mu_1^2 + a_2\mu_2^2)^2 \times (c_1\mu_1^2 + c_2\mu_2^2) + c_4^{(1)}\mu_1^4 + c_4^{(2)}\mu_2^4, \quad (12)$$

where $b = T_c^0$, $a_1 = \tilde{a}_1/b$ and $a_2 = \tilde{a}_2/b$. Both a_1 and a_2 have the dimension of b^{-1} (GeV). The free energy will be

measured in units of GeV^4 . It is worth mentioning that the components of the thermodynamic metric tensor are in units of GeV^2 , hence the thermodynamic curvature is in units of GeV^4 , and the chemical potentials μ_i are in the units of GeV .

The above expression for the free energy is now only a function of the two quark chemical potentials (μ_1, μ_2), since the temperature dependence has been traded off in favor of the quark chemical potentials. The validity of the free energy $F(\mu_1, \mu_2)$ as depicted in the Eq.(12), and thus all the quantities derived from it depends upon the condition whether the chemical potentials, μ_1 and μ_2 satisfy: $|\mu_i| < T_c^0$ ($i=1,2$). We shall show later, the variation of μ_1 and μ_2 are within the range of validity.

The underlying covariant thermodynamic geometry arising from this free energy of hot QCD can be determined by employing the general formalism quoted in the previous section, which we do systematically in Section 4. Let us first discuss how one incorporates thermal fluctuations into the free energy and later on we shall study the contributions to the geometric structure of free energy.

Let us now compute the contribution to the thermodynamic geometry from the thermal fluctuations. Let us consider case (A) for the 2-flavor QCD first. The free energy defined as the negative logarithm of the partition function takes the general polynomial form

$$F(\mu_1, \mu_2) := a_0 + c_1 \left(\frac{\mu_1}{T} \right)^2 + c_2 \left(\frac{\mu_2}{T} \right)^2. \quad (13)$$

Since the specific heat as the thermodynamic parameters at constant volume may be defined as the second partial derivative of the free energy with respect to the temperature, this enforces that the associated leading order free energy with the inclusion of the thermal fluctuations after substituting for T_C as a function of chemical potentials reads

$$F(\mu_1, \mu_2) := a_0 + \frac{c_1\mu_1^2 + c_2\mu_2^2}{(b + a_1\mu_1^2 + a_2\mu_2^2)^2} + \frac{1}{2} \ln \left(\frac{c_1\mu_1^2 + c_2\mu_2^2}{(b + a_1\mu_1^2 + a_2\mu_2^2)^2} \right). \quad (14)$$

Let us turn our attention to explore the thermodynamic geometry of the equilibrium configuration space of the hot QCD, arising from the free energy expression at the various order perturbative contributions as well as that of the thermal fluctuations at the leading order free energy. In order to analyze the geometric nature of the hot QCD, we shall focus our attention on the realistic values characterizing certain specific phases of the QCD. In particular, the examples of interest are the case of two flavor QCD or that of 3-flavor QCD. As the exact expression for the components of the metric tensors, associated determinants and that of the scalar curvatures are rather involved with general coefficients, thus we shall provide the geometric expressions only for the realistic parameters of the free energy which describes the present nature in hot QCD near the T_C . For simplicity, we have not

explicitly considered the mass of the quarks but on general ground, the geometric conclusions may be expected to retain the same conclusions. Moreover, this is an interesting path to pursue and, for instance by arguments similar to the one given above we can conclude that the general results with the inclusion of the thermal fluctuations agree with the results for arbitrary perturbatively corrected free energy in the framework of the theories of the quasi-particles. We shall now proceed to study the thermodynamic geometry in Case(A) and Case(B) one by one in the 2- and 3-flavor QCD. We shall henceforth suppress the units of the thermodynamic metric (GeV^2) and thermodynamic curvature (GeV^4).

IV. 2-FLAVOR QCD

In this section, we shall present the essential features of thermodynamic geometries and thereby put them into effect for the 2-flavor hot QCD. In particular, we focus our attention on the geometric nature of QCD in the neighborhood of T_C with given quark chemical potentials introduced in the framework of quasi-particle theories. As stated earlier the thermodynamic metric in the chemical potential space is given by the Hessian matrix of the free energy with respect to the intensive variables which in this case are the two distinct chemical potentials carried by the quarks.

A. Case(A)

Considering Eq.12 in the neighborhood of T_C and substituting for T_C as function of μ_1 and μ_2 , one obtains the following expression:

$$F(\mu_1, \mu_2) := a_0(b + a_1\mu_1^2 + a_2\mu_2^2)^4 + (b + a_1\mu_1^2 + a_2\mu_2^2)^2 \times (c_1\mu_1^2 + c_2\mu_2^2). \quad (15)$$

To obtain the thermodynamic metric tensor in the chemical potential space, we employ the formula in Eq. 2, which leads to the following polynomial expression for the components of the metric tensor:

$$\begin{aligned} g_{\mu_1, \mu_1} &= 1.12\mu_2^4 + 5.60\mu_1^4 + 6.72\mu_1^2\mu_2^2 - 6.48\mu_1^4\mu_2^2 \\ &\quad - 3.89\mu_1^2\mu_2^4 - 2.21\mu_1^2 - 0.74\mu_2^2 + 0.13 \\ &\quad - 3.02\mu_1^6 - 0.43\mu_2^6, \\ g_{\mu_1, \mu_2} &= -1.48\mu_1\mu_2 + 4.48\mu_1^3\mu_2 + 4.48\mu_1\mu_2^3 \\ &\quad - 2.59\mu_1^5\mu_2 - 2.59\mu_1\mu_2^5 - 5.18\mu_1^3\mu_2^3, \\ g_{\mu_2, \mu_2} &= 1.12\mu_1^4 + 5.60\mu_2^4 + 6.72\mu_1^2\mu_2^2 - 6.48\mu_1^2\mu_2^4 \\ &\quad - 3.89\mu_1^4\mu_2^2 - 2.21\mu_2^2 - 0.74\mu_1^2 + 0.13 \\ &\quad - 3.02\mu_2^6 - 0.43\mu_1^6. \end{aligned} \quad (16)$$

We thus see that the components of metric functions indeed satisfy (i) $g_{\mu_1, \mu_1}(\mu_1, \mu_2) = g_{\mu_2, \mu_2}(\mu_2, \mu_1)$ and (ii)

$g_{\mu_1, \mu_2}(\mu_1, \mu_2) = g_{\mu_1, \mu_2}(\mu_2, \mu_1)$. The thermodynamic geometry predictions thus obtained indicate that the nature of two point correlation functions of such 2-flavor QCD must satisfy (i) and (ii). In particular, this determines the nature of associated quark number that the susceptibility tensor satisfies: $\chi_{ij}(\mu_1, \mu_2) = \chi_{ji}(\mu_2, \mu_1) = \chi$ and $\chi_{ij}(\mu_1, \mu_2) = \chi_{ij}(\mu_2, \mu_1)$, where i, j are the flavor indices associated with the 2-flavor QCD configuration, see for a phenomenological example [1]. Furthermore, the determinant of the metric tensor turns out to be polynomial, and can be given in compact notations as follows

$$g(\mu_1, \mu_2) = \sum_{k,l=0|k+l \leq 6}^6 a_{k,l}^A \mu_1^{2k} \mu_2^{2l} \quad (17)$$

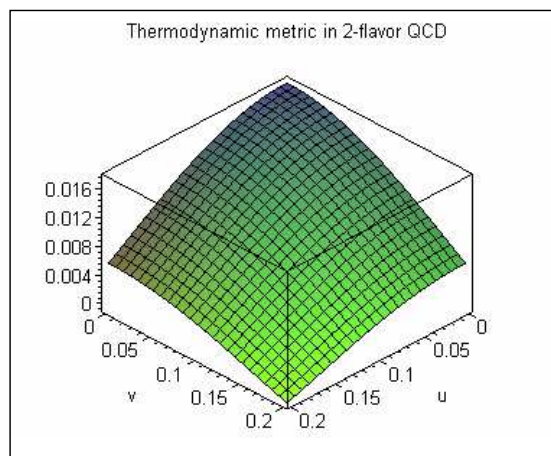


FIG. 1. The determinant of the thermodynamic metric in 2-flavor QCD in the chemical potentials surface. Note that we measure the chemical potential in GeV.

Employing the formula displayed in Eq.4, we obtain the thermodynamic curvature which is also a polynomial in μ_1 and μ_2 . It can be written as

$$R(\mu_1, \mu_2) = -\frac{4}{g^2} \sum_{k,l=0|k+l \leq 7}^7 b_{k,l}^A \mu_1^{2k} \mu_2^{2l}. \quad (18)$$

The determinants of the thermodynamic metric and curvature in the chemical potential space are shown in Figs 1 and 2 respectively. We denote $(\mu_1, \mu_2) \equiv (u, v)$, and henceforth focus our attention in the physically interesting domain near T_C , where both u and v lie between 0.0 to 0.2. In this case, we see that there are two distinct curves of certain bumps of varying lengths whose size depends on the domain chosen in the (u, v) space. The significance of these bumps is that they show thermodynamical interactions in the underlying system. For the determinant of the metric tensor, when plotted

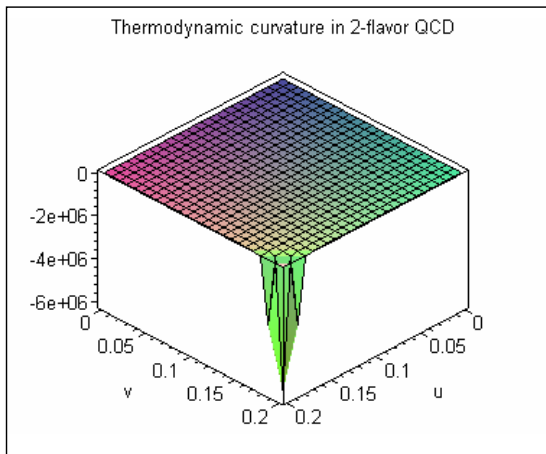


FIG. 2. Thermodynamic curvature in 2-flavor QCD in the chemical potentials surface. Note that we measure the chemical potential in GeV.

against the chemical potentials, we find that it is a regular increasing function of the chemical potentials in the considered physical domains of hot QCD.

B. Case(B)

Considering the expansion of the free energy given in Eq. 12, and employing Eq. 2 for non vanishing c_4^1, c_4^2 defined in Eq. 9, the following expression for the components of the metric tensor may be obtained:

$$\begin{aligned}
 g_{\mu_1, \mu_1} &= 6.72\mu_1^2\mu_2^2 - 2.52\mu_1^2 - 0.74\mu_2^2 + 0.13 + 5.60\mu_1^4 \\
 &\quad + 1.12\mu_2^4 - 3.02\mu_1^6 - 0.43\mu_2^6 - 6.48\mu_1^4\mu_2^2 \\
 &\quad - 3.89\mu_1^2\mu_2^4, \\
 g_{\mu_1, \mu_2} &= -1.48\mu_1\mu_2 + 4.48\mu_1^3\mu_2 + 4.48\mu_1\mu_2^3 - 2.59\mu_1^5\mu_2 \\
 &\quad - 2.59\mu_1\mu_2^5 - 5.18\mu_1^3\mu_2^3, \\
 g_{\mu_2, \mu_2} &= 6.72\mu_1^2\mu_2^2 - 2.52\mu_2^2 - 0.74\mu_1^2 + 0.13 + 5.60\mu_2^4 \\
 &\quad + 1.12\mu_1^4 - 3.02\mu_2^6 - 0.43\mu_1^6 - 6.48\mu_1^2\mu_2^4 \\
 &\quad - 3.89\mu_1^4\mu_2^2.
 \end{aligned} \tag{19}$$

We see further that in this Case(B), the symmetry ($\mu_i \rightarrow -\mu_i$) and exchange symmetry of the thermodynamic geometry remains conserved as that in the Case(A). This in fact remains true in general for any symmetric function $F(\mu_1, \mu_2)$ whose Hessian matrix defines the metric tensor of the underlying intrinsic Riemannian manifold. The determinant of the metric tensor turns out to be a polynomial function in the chemical potentials $\{\mu_1, \mu_2\}$, which in turn is given in the compact notations as

$$g(\mu_1, \mu_2) = \sum_{k,l|k+l=0 \leq 6} a_{k,l}^B \mu_1^{2l} \mu_2^{2k} \tag{20}$$

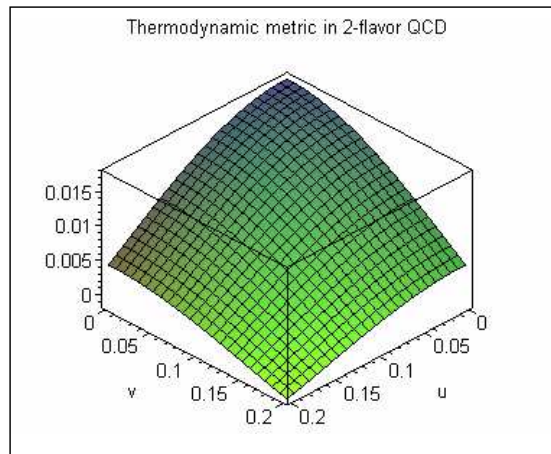


FIG. 3. The determinant of the thermodynamic metric in 2-flavor QCD as a surface plotted against the chemical potentials. Note that we measure the chemical potential in GeV.

$$R(\mu_1, \mu_2) = -\frac{4}{g^2} \sum_{k,l=0|k+l \leq 7} b_{k,l}^B \mu_1^{2k} \mu_2^{2l} \tag{21}$$

We see that the determinant of the metric tensor remains non-zero in the small chemical potential limit and thus defines a non-degenerate thermodynamic geometry near T_C . Finally, we may easily obtain the underlying thermodynamic curvature which also having a polynomial form and can be written as,

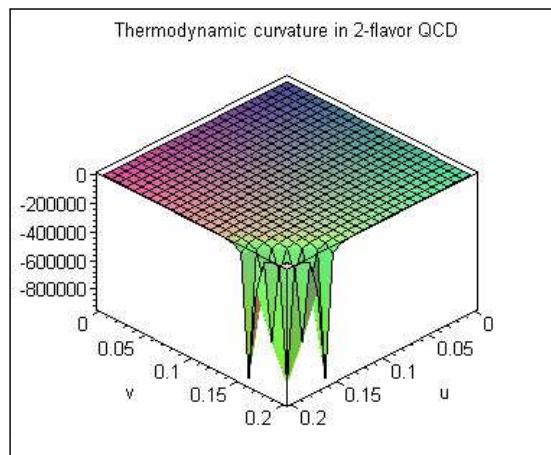


FIG. 4. Thermodynamic curvature in 2-flavor QCD in the chemical potentials surface. Note that we measure the chemical potentials in GeV.

The behavior of g and R as a function quark chemical potentials in Case (B) for 2-flavor QCD are shown in Figs.3 and 4. Here the conclusions to be drawn in the range of the chemical potentials considered

in the previous case remain the same, except for the fact that the curves of the interactions are aligned with an enhanced magnitude, while the shape of the determinant of the metric tensor plotted against the chemical potentials remains (exactly) the same as in the previous case.

We see however that the components of the metric tensor at zero chemical potentials take the values $g_{\mu_1, \mu_1} = a_{0,0}^B \equiv 0.13 = g_{\mu_2, \mu_2}$ and $g_{\mu_1, \mu_2} = 0$, which effectively describe nothing more than the diagonal and, respectively, off diagonal quark susceptibility tensors. We find further that the determinant of the metric tensor reduces to the value of $g = 0.02$ at zero chemical potentials, while the scalar curvature becomes zero at this point and thus the underlying statistical system at this point becomes non-interacting. We further see that these diagonal and off diagonal quark susceptibility tensors, as well as the determinant of the metric tensor and the scalar curvature at zero chemical potentials, remain the same under the $(\frac{\mu}{T})^4$ -contributions.

In the case of the 2-flavor QCD free energy, we note that the degree of the determinant of the thermodynamic geometry in the chemical potential space remains intact for the Case(B) as that of the Case(A). We further see that the associated thermodynamic curvature never diverges for any values of the chemical potentials, and tends to a vanishingly small quantity when either one of the chemical potential corresponds to a large value. Our predictions can thus easily be generalized to the case when the free energy may be expressed as a finite polynomial expression of two chemical potentials. We have further noticed that the thermodynamic geometry of the free energy preserves all the symmetries of the free energy. Let us now proceed to study the effects of thermal fluctuations to the thermodynamic geometry of case (A) in 2-flavor QCD.

C. Thermal Fluctuations

We will now discuss the thermodynamic geometry of hot QCD with the inclusion of thermal fluctuations about an equilibrium. As it is well known, any thermodynamical system considered as a canonical ensemble has logarithmic and polynomial contributions to the free energy [3]. These considerations apply as well to quasi-particles models of QCD, and the specific forms of the logarithmic and polynomial contributions may easily be calculated for a wide class of particle theories. In order to analyze essential geometric nature of hot QCD under thermal contributions, we shall consider the case of the quadratic corrected free energy. Further it is straightforward to see that the case of quartic corrected free energy in this framework leaves the qualitative nature of results untouched. This approximation is valid only in the regime where thermal fluctuations are much larger than quantum fluctuations.

With the above consideration in the leading order quadratic approximation, the corresponding free energy

of two flavor QCD reads

$$F(\mu_1, \mu_2) = a_0 + \frac{c_1\mu_1^2 + c_2\mu_2^2}{(b + a_1\mu_1^2 + a_2\mu_2^2)^2} + \frac{1}{2} \ln\left(\frac{c_1\mu_1^2 + c_2\mu_2^2}{(b + a_1\mu_1^2 + a_2\mu_2^2)^2}\right). \quad (22)$$

Employing the formula to determine the metric tensor and thermodynamic curvature displayed in Eqs.2, the components are the metric tensor in the scale of 10^{10} come out to be

$$\begin{aligned} g_{\mu_1, \mu_1} &= \{-0.17(\mu_1^2 - \mu_2^2) - 1.33(\mu_1^{10} - \mu_1^{10}) \\ &\quad + 9.96\mu_2^8 - 36.26\mu_1^8 - 3.55\mu_2^4 - 5.82\mu_1^4 \\ &\quad + 2.67(\mu_2^6\mu_1^4 - \mu_1^6\mu_2^4) - 102.80(\mu_2^2\mu_1^4 - 0.5\mu_1^2\mu_2^4) \\ &\quad - 78.93\mu_1^4\mu_2^4 - 36.27\mu_1^8 - 51.40\mu_1^6 - 5.82\mu_1^4 \\ &\quad - 1.33\mu_1^{10} - 6.38\mu_2^6\mu_1^2 - 98.86\mu_2^2\mu_1^6 \\ &\quad - 4.00(\mu_2^2\mu_1^8 - \mu_1^2\mu_2^8) - 9.37\mu_1^2\mu_2^2\} \\ &\quad \times (-203 + 340\mu_1^2 + 340\mu_2^2)^{-4}(\mu_1^2 + \mu_2^2)^{-2}, \\ g_{\mu_1, \mu_2} &= 2\mu_1\mu_2\{1.13(\mu_1^2 + \mu_2^2) + 23.12(\mu_2^6 + \mu_1^6) \\ &\quad + 1.33(\mu_1^8 + \mu_2^8) + 51.40(0.50\mu_1^4 + \mu_2^4) \\ &\quad + 69.36(\mu_2^2\mu_1^4 + \mu_1^2\mu_2^4)8.01(\mu_1^4 + \mu_2^4) \\ &\quad + 5.34(\mu_1^2\mu_2^6 + \mu_1^6\mu_2^2) + 51.40\mu_1^2\mu_2^2 - 0.17\} \\ &\quad \times (-203 + 340\mu_1^2 + 340\mu_2^2)^{-4}(\mu_1^2 + \mu_2^2)^{-2}, \\ g_{\mu_2, \mu_2} &= \{-0.17(\mu_2^2 - \mu_1^2) - 1.33(\mu_1^{10} - \mu_2^{10}) \\ &\quad + 9.96\mu_1^8 - 36.26\mu_1^8 - 3.55\mu_1^4 - 5.82\mu_1^4 \\ &\quad + 2.67(\mu_1^6\mu_2^4 - \mu_2^6\mu_1^4) - 102.80(\mu_1^2\mu_2^4 \\ &\quad - 0.5\mu_2^2\mu_1^4) - 78.93\mu_2^4\mu_1^4 - 36.27\mu_2^8 \\ &\quad - 51.40\mu_2^6 - 5.82\mu_2^4 - 1.33\mu_2^{10} - 6.38\mu_1^6\mu_2^2 \\ &\quad - 98.86\mu_1^2\mu_2^6 - 4.00(\mu_1^2\mu_2^8 - \mu_2^2\mu_1^8) \\ &\quad - 9.37\mu_2^2\mu_1^2\} \times (\mu_1^2 + \mu_2^2)^{-2} \\ &\quad (-203 + 340\mu_1^2 + 340\mu_2^2)^{-4}. \end{aligned} \quad (23)$$

It is thus evident that the symmetry of the metric tensor remains preserved under thermal fluctuations. In this case, after incorporating the Log contributions to the free energy in the case of 2-flavor QCD, we obtain the following positive definite expressions for the determinant of the thermodynamic metric:

$$g(\mu_1, \mu_2) = 4 \frac{\sum_{k,l=0}^7 a_{l,k}^C \mu_1^{2k} \mu_2^{2l}}{(\mu_1^2 + \mu_2^2)^2 (0.20 - 0.34(\mu_1^2 - \mu_2^2))^7} \quad (24)$$

We see in this case again that the thermodynamic curvature turns out in the form of the ratio of two polynomial expressions, which may be written as

$$R(\mu_1, \mu_2) = -\frac{4}{g^2} (0.20 - 0.34(\mu_1^2 + \mu_2^2)) \times \sum_{k,l=0}^{12} b_{k,l}^C \mu_1^{2k} \mu_2^{2l}, \quad (25)$$

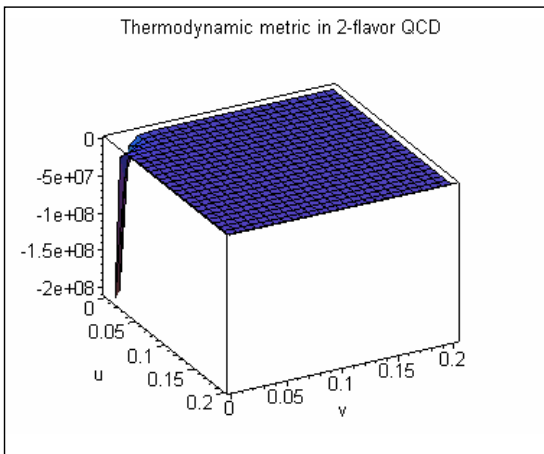


FIG. 5. The determinant of the metric tensor in 2-flavor QCD under thermal corrections in the chemical potentials surface. Note that we measure the chemical potential in GeV.

where the coefficients $\{a_{i,j}\}$ of the polynomial expression appearing in the numerator may easily be tracked from the corresponding points on the figure 6. In this case, we should note that the determinant of the metric tensor plotted against the chemical potentials becomes a smoother function in comparison to that of the case without logarithmic correction. However, we observe that it reaches a magnitude of 10^9 near the $(u, v) = (0.2, 0.2)$. Further, we find that the domain of the interaction has shifted towards the origin. In particular, we see that such interactions are only present in the chemical potentials range $0.1 < \mu_i < 0.2$.

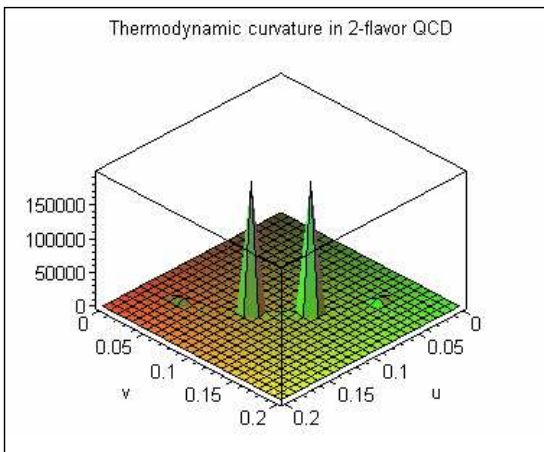


FIG. 6. Thermodynamic curvature in 2-flavor QCD under thermal corrections in the chemical potentials surface. Note that we measure the chemical potential in GeV.

Finally, we wish to point out a general feature of the above geometric considerations, i.e. that any polynomial free energy after including the logarithmic contributions

is going to generate certain bump(s) in the intrinsic Riemannian space of chemical potentials for a given non-zero T_C around the equilibrium QCD thermodynamic configuration. Furthermore, following our general procedure it may explicitly be verified, in the same way as in the cases of quadratic or quartic contributions to the free energy, that the logarithmic contributions to the free energy do not spoil the symmetry of the determinant and that of the associated scalar curvature of the intrinsic space spanned by the quasi-particle chemical potentials. Such symmetries are indeed the artifact of the choice of the parameters appearing in the corresponding free energy such that they correspond to the symmetric free energy in the chemical potentials. Due to the inherent symmetries in the definition of the quasi-particle free energies, it is possible in principle that we can give up manifestly invariant expressions for the determinants and the scalar curvatures. In particular, we find that for all quasi-particle free energy $F(\mu_1, \mu_2) := \sum_{i,j} a_{i,j} \mu_1^i \mu_2^j$ with $a_{i,j} = a_{j,i}$, it turns out that the determinant and associated scalar curvature of the intrinsic Riemannian manifold as a function of the quark chemical potentials are symmetric functions $g(\mu_1, \mu_2) = g(\mu_2, \mu_1)$ and $R(\mu_1, \mu_2) = R(\mu_2, \mu_1)$ of the chemical potentials.

V. 3-FLAVOR QCD

As in the previous section, we shall analyze the free energy as a function of quark chemical potentials with or without thermal corrections, and thereby systematically explore the covariant metric tensor, determinant and scalar curvature of the thermodynamic geometry of 3-flavor QCD.

A. Case(A)

In what follows next in this subsection, we present the geometric analysis for the realistic quasi-particle model of QCD near the T_C . The thermodynamic geometry of interest may thus easily be obtained, as before, from the Hessian matrix of the free energy with respect to the quark chemical potentials. In this case the components of the metric tensor reduce to

$$\begin{aligned}
 g_{\mu_1, \mu_1} &= -7.59\mu_1^2 - 2.30\mu_2^2 + 0.26 + 33.76\mu_1^4 \\
 &\quad + 6.08\mu_2^4 - 32.50\mu_1^6 + 38.51\mu_1^2\mu_2^2 \\
 &\quad - 69.65\mu_1^4\mu_2^2 - 41.79\mu_1^2\mu_2^4 - 4.64\mu_2^6, \\
 g_{\mu_1, \mu_2} &= -4.60\mu_1\mu_2 + 25.67\mu_1^3\mu_2 + 24.33\mu_1\mu_2^3 \\
 &\quad - 27.86\mu_1^5\mu_2 - 55.72\mu_1^3\mu_2^3 - 27.86\mu_1\mu_2^5, \\
 g_{\mu_2, \mu_2} &= -6.22\mu_1^2 - 2.30\mu_2^2 + 0.22 + 6.41\mu_1^4 \\
 &\quad + 28.75\mu_2^4 - 4.64\mu_1^6 + 36.50\mu_1^2\mu_2^2 \\
 &\quad - 41.79\mu_1^4\mu_2^2 - 69.65\mu_1^2\mu_2^4 - 32.50\mu_2^6. \quad (26)
 \end{aligned}$$

We see further that the components of the metric tensor at zero chemical potentials take the values $g_{\mu_1, \mu_1} = 0.26$, $g_{\mu_2, \mu_2} = 0.22$ and $g_{\mu_1, \mu_2} = 0$, which in effect respectively describe the diagonal and off diagonal quark susceptibility tensors. We further find that the determinant of the metric tensor reduces to the value of $g = 0.06$ at zero chemical potentials, while the scalar curvature vanishes at this point and thus the underlying statistical system approaches a non-interacting system. On the other hand, the determinant of the metric for this 3 flavor case is as follows:

$$g(\mu_1, \mu_2) = \sum_{k,l=0|k+l \leq 6}^6 \tilde{a}_{k,l}^A \mu_1^{2l} \mu_2^{2k} \quad (27)$$

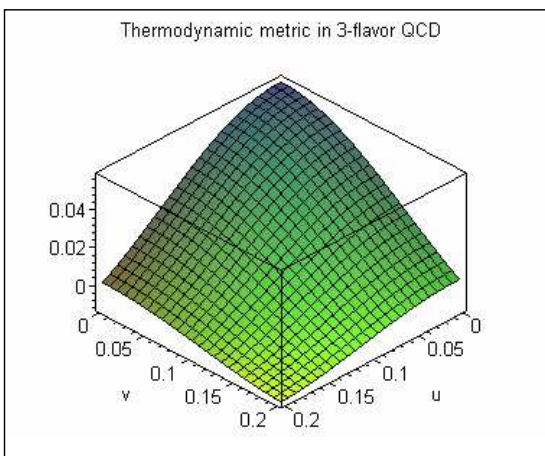


FIG. 7. The determinant of the thermodynamic metric in 3-flavor QCD in the chemical potentials surface. Note that we measure the chemical potential in GeV.

In this case we see that $g(\mu_1, \mu_2) \neq g(\mu_2, \mu_1)$, which follows from the fact that the 3-flavor QCD free energy (displayed in Eq.12) is not symmetric under the exchange in the chemical potentials. The same remains true for the associated curvature, which may be seen from

$$R(\mu_1, \mu_2) = -\frac{4}{g^2} \sum_{k,l=0|k+l \leq 7}^7 \tilde{b}_{k,l}^A \mu_1^{2k} \mu_2^{2l} \quad (28)$$

From Figs.7 and 8, we see that the determinant of the metric tensor plotted against the chemical potentials shows two lines of minima and the maximum lying in between the minima occurs when either one of the chemical potentials reaches a non-zero constant value, while the other is fixed at the origin. In this case we further see that there are two distinct bumps of varying heights instead of the curves of interactions. The height of the bumps depends on the domain chosen in the (u, v) space.

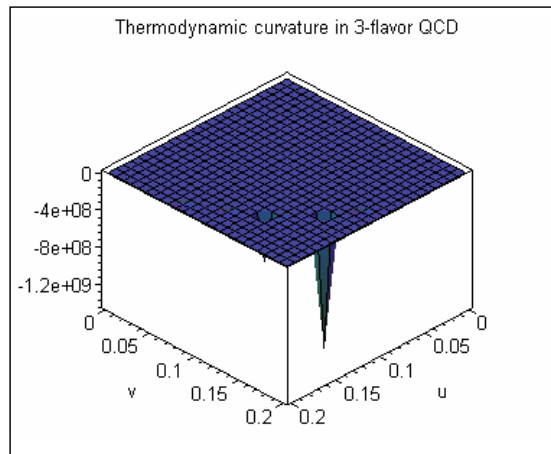


FIG. 8. Thermodynamic curvature in 3-flavor QCD in the chemical potentials surface. Note that we measure the chemical potential in GeV.

The significance of these bumps is that they show thermodynamical interactions in the system of the 3-flavor QCD.

B. Case(B)

In this subsection, we shall investigate the thermodynamic geometry corresponding to the free energy given by Eq.8. It turns out here that the components of the metric tensor thus obtained are as follows:

$$\begin{aligned} g_{\mu_1, \mu_1} &= -38.51\mu_1^2\mu_2^2 + 6.08\mu_2^4 - 69.65\mu_1^4\mu_2^2 \\ &\quad - 8.20\mu_1^2 - 2.30\mu_2^2 + 0.61 + 33.76\mu_1^4 \\ &\quad - 41.79\mu_1^2\mu_2^4 - 32.50\mu_1^6 - 4.64\mu_2^6, \\ g_{\mu_1, \mu_2} &= -4.60\mu_1\mu_2 + 25.67\mu_1^3\mu_2 + 24.33\mu_1\mu_2^3 \\ &\quad - 27.86\mu_1^5\mu_2 - 55.72\mu_1^3\mu_2^3 - 27.86\mu_1\mu_2^5, \\ g_{\mu_2, \mu_2} &= -36.51\mu_1^2\mu_2^2 + 28.75\mu_2^4 - 41.79\mu_1^4\mu_2^2 \\ &\quad - 2.30\mu_1^2 - 6.53\mu_2^2 + 0.22 + 3.42\mu_1^4 \\ &\quad - 69.65\mu_1^2\mu_2^4 - 4.64\mu_1^6 - 32.50\mu_2^6. \end{aligned} \quad (29)$$

In this case the conclusion to be drawn in the range of the chemical potentials considered in the previous case remains the same, except the fact that the number of bumps is increased, which thus indicates stronger interactions in the internal space of the quark chemical potentials, while the shape of the determinant of the metric tensor plotted against the chemical potentials is a bit flatter near the $(u, v) = (0.2, 0.2)$ than the previous case. The determinant of the metric tensor turns out to be polynomial

$$g(\mu_1, \mu_2) = \sum_{k,l=0|k+l \leq 6}^6 \tilde{a}_{k,l}^B \mu_1^{2l} \mu_2^{2k} \quad (30)$$

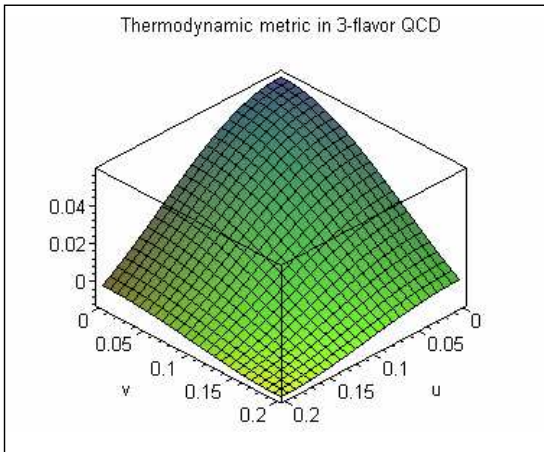


FIG. 9. The determinant of the metric tensor in 3-flavor QCD as a function of the chemical potentials. Note that we measure the chemical potential in GeV.

Note further in this case, we again see that $g(\mu_1, \mu_2) \neq g(\mu_2, \mu_1)$, which follows directly from the fact that the underlying free energy with $(\frac{\mu}{T})^4$ -contributions (displayed in Eq.8) remains non-symmetric under the exchange of the quarks chemical potentials. Thus the same remains true for the associated curvature as the polynomial ratio of the Riemann tensor and the determinant of the metric tensor, which turns out to be given by

$$R(\mu_1, \mu_2) = -\frac{4}{g^2} \sum_{k,l=0|k+l \leq 7}^7 \tilde{b}_{k,l}^B \mu_1^{2k} \mu_2^{2l} \quad (31)$$

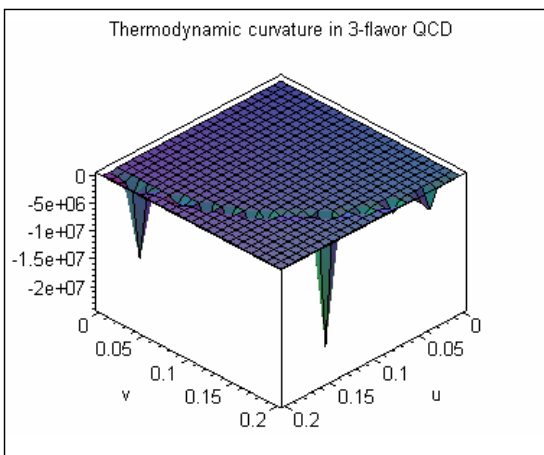


FIG. 10. Thermodynamic curvature in 2-flavor QCD in the chemical potentials surface in case B. Note that we measure the chemical potential in GeV.

In these cases when the free energy may be treated as a function of the chemical potentials, we see that the thermodynamic space spanned by the chemical potentials remains completely regular except at those points for which the determinant of the metric tensor vanishes on the intrinsic manifold. This intrinsic space of the chemical potentials thus turns out to be a well-defined, stable configuration for all $\{\mu_1, \mu_2\}$ such that the the determinant of the associated metric tensor remains positive definite in the domain of interest. We see in this case that the underlying diagonal quark susceptibility tensor does not remain the same at zero chemical potentials, and in particular, we find that $g_{\mu_1, \mu_1} = 0.61$, $g_{\mu_2, \mu_2} = 0.22$ and $g_{\mu_1, \mu_2} = 0$ while the determinants of the metric tensor and the scalar curvature remain the same under the $(\frac{\mu}{T})^4$ -contributions at zero chemical potentials.

C. Thermal Fluctuations

We will now discuss the thermodynamic properties of 3-flavor QCD under thermal fluctuations, treating the system as a well-defined ensemble. We allow for small thermal fluctuations in the system considered, and study the thermodynamic geometry of 3-flavor QCD in the lines with our treatment of the usual two flavor QCD described earlier in the previous section. For simplicity we shall work in the leading order approximation with the corresponding free energy as that of two flavor QCD, with the understanding that the parameters appearing in the free energy are given as that of the quadratic case of 3-flavor QCD. A straightforward computation yields that the components of the metric tensor in the scale of 10^{10} read

$$\begin{aligned} g_{\mu_1, \mu_1} &= -2(-197 + 578\mu_1^2 + 578\mu_2^2)^{-4}(2\mu_1^2 + \mu_2^2)^{-2} \\ &\quad \{7.50\mu_2^6 + 3.80\mu_2^8 + 0.30\mu_1^2 - 0.15\mu_2^2 \\ &\quad - 2.56\mu_2^4 + 182.75\mu_1^4\mu_2^4 - 28.69\mu_1^2\mu_2^4 \\ &\quad + 78.13\mu_1^6\mu_2^4 - 22.32\mu_1^{10} - 416.12\mu_1^8 \\ &\quad - 343.63\mu_1^6 - 11.16\mu_1^8\mu_2^2 - 91.30\mu_1^6\mu_2^2 \\ &\quad - 19.06\mu_1^2\mu_2^2 - 274.74\mu_1^4\mu_2^2 - 20.83\mu_1^4 \\ &\quad + 62.18\mu_1^2\mu_2^6 + 100.45\mu_1^4\mu_2^6 + 33.48\mu_1^2\mu_2^8\}, \\ g_{\mu_1, \mu_2} &= 4\mu_1\mu_2(-197 + 578\mu_1^2 + 578\mu_2^2)^{-4}(2\mu_1^2 + \mu_2^2)^{-2} \\ &\quad \{7.61\mu_2^6 + 1.77\mu_1^2 + 1.77\mu_2^2 + 27.68\mu_2^4 \\ &\quad + 78.13\mu_1^4\mu_2^4 + 107.83\mu_1^2\mu_2^4 + 33.48\mu_1^8 \\ &\quad + 385.68\mu_1^6 + 89.29\mu_1^6\mu_2^2 + 126.27\mu_1^2\mu_2^2 \\ &\quad + 385.68\mu_1^4\mu_2^2 + 143.05\mu_1^4 + 22.32\mu_1^2\mu_2^6 \\ &\quad - 0.15\}, \\ g_{\mu_2, \mu_2} &= (-197 + 578\mu_1^2 + 578\mu_2^2)^{-4}(2\mu_1^2 + \mu_2^2)^{-2} \\ &\quad \{80.72\mu_2^6 + 107.83\mu_2^8 + 0.30\mu_2^2 - 0.15\mu_2^4 \\ &\quad - 11.16\mu_2^{10} + 6.53\mu_2^4 + 1911.89\mu_1^4\mu_2^4 \\ &\quad + 368.99\mu_1^2\mu_2^4 + 66.97\mu_1^4\mu_2^6 - 69.97\mu_1^{10} \\ &\quad - 340.04\mu_1^8 + 75.53\mu_1^6 - 100.54\mu_1^8\mu_2^2 \} \end{aligned}$$

$$\begin{aligned}
& +1278.78\mu_1^6\mu_2^2 + 17.29\mu_1^2\mu_2^2 + 437.31\mu_1^4\mu_2^2 \\
& +15.52\mu_1^4 + 801.80\mu_1^2\mu_2^6 + 178.58\mu_1^4\mu_2^6 \\
& +89.29\mu_1^8\mu_2^2\}.
\end{aligned} \tag{32}$$

The determinant of the metric tensor turns out to be given by the following polynomial expression:

$$\begin{aligned}
g(\mu_1, \mu_2) &= \left((0.197 - 0.578(\mu_1^2 + \mu_2^2))^7 (\mu_1^2 + 0.50\mu_2^2)^2 \right) \\
&\times \sum_{k,l=0|k+l\leq 12}^{12} \tilde{b}_{k,l}^C \mu_1^{2k} \mu_2^{2l},
\end{aligned} \tag{33}$$

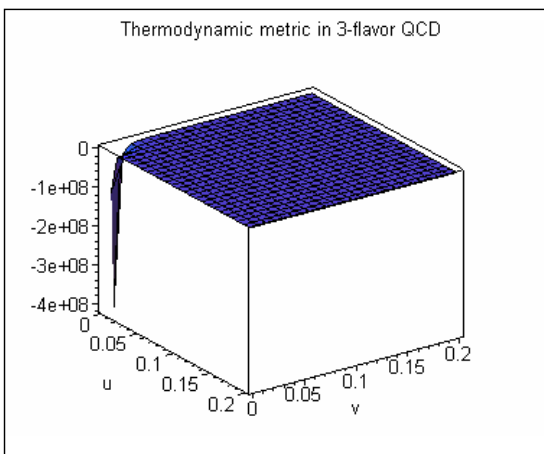


FIG. 11. The determinant of the metric tensor in 3-flavor QCD in the chemical potentials surface when the thermal contributions are included. Note that we measure the chemical potential in GeV.

In this case, we see that the determinant of the metric tensor plotted against the chemical potentials acquires two finite size bumps which were absent in the case without thermal corrections. Again the height of the bumps depends on the location being chosen. Furthermore, we find that the domain of the interaction has shifted towards the origin, as in the previously treated case of 2-flavor QCD. In particular, we see that there are two bumps of interactions present near the value of either chemical potentials $\mu_i = 0.1$. However, we observe that the strength of the interaction depends on the exact location chosen in the internal space, for example it may become as high as 10^4 or as small as 10^2 near the $(u, v) = (0.1, 0.1)$.

In this case again it turns out that the thermodynamic curvature may be written in the same form as the ratio of two polynomial expressions, and in particular we find that this curvature is given by

$$R(\mu_1, \mu_2) = -\frac{4}{g^2} (0.197 - 0.578(\mu_1^2 + \mu_2^2))$$

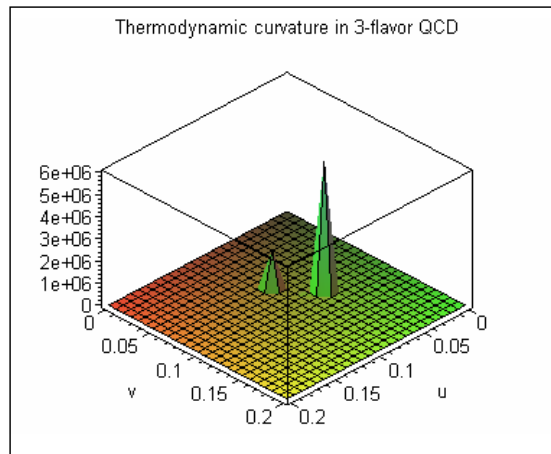


FIG. 12. Thermodynamic curvature in 3-flavor QCD in the chemical potentials surface when the thermal contributions are included. Note that we measure the chemical potential in GeV.

$$\sum_{\{k,l=0|k+l\leq 12\}}^{12} \tilde{b}_{k,l}^C \mu_1^{2l} \mu_2^{2k}, \tag{34}$$

where the associated coefficients $\{\tilde{b}_{k,l}\}$ of the Riemann tensor appearing in the numerator of the scalar curvature may easily be read out from the corresponding Fig. 12. Thus, in this section once again one can always find from the general considerations of the intrinsic Riemannian geometry as in the case of 2-flavor QCD that for any given polynomial free energy after including the logarithmic contributions there exist certain bump(s) in the associated intrinsic Riemannian space.

VI. DISCUSSION AND CONCLUSION

In this paper we have introduced an intrinsic geometric notion to QCD thermodynamics, and thereby it has been applied to study the behavior of 2-flavor and 3-flavor QCD in several simple thermodynamic considerations. The free energy of the 2-flavor, as well as that of the 3-flavor QCD, with or without logarithmic contributions under thermal fluctuations, indicate an intriguing relationships between the geometrical concepts of QCD thermodynamics, and in particular, the scalar curvature of the underlying metric tensor to the correlation volume. Thus the physical concepts of a phase transition(s), if any, as well as the geometric apprehension of the quasi-particles, non-ideal interactions are divulged. For 2-flavor QCD as a thermodynamic system with two distinct quark chemical potentials, the associated quarks susceptibility tensors may consequently be defined as the components of the thermodynamic metric tensor arising from the Hessian of the hot QCD free energy and thus represent the scalar curvature of the underlying geometry from the viewpoint of the statistical theory of quark

states. We have explicitly determined such notions for a few simple cases, in particular for the 2-flavor and the 3-flavor theories, and it turns out that they indicate certain physical behavior in the lieu of “*macroscopic/microscopic duality*” relation(s), which are indeed in close connection with the “*AdS/CFT correspondence*” via an associated fermion number density of the underlying effective field theory. In fact, this study provides convincing examples that the intrinsic geometric approach analyzes the thermodynamics of hot QCD systems from the perspective of microscopic theory and thus can be applied to actually divulge important physical and chemical behavior of the quasi-particles.

A. Thermodynamic Parameters

We have shown that the covariant intrinsic geometric notion about an equilibrium thermodynamics configuration, when applied to the 2-flavor and 3-flavor quasi-particle QCD models considered as thermodynamic systems, provided that they are an integral part of the environment with which they are treated to be in equilibrium, in the framework of an underlying ensemble theory, indicates in both cases a well-defined, curved, regular intrinsic Riemannian manifold. Hence, the study of the equilibrium thermodynamic geometry as an intrinsic manifold arising from quasi-particles and the associated scalar curvature have led us to interesting insights into phase transitions and critical phenomena, if any, for such quasi-particles. However, it may be mentioned that a thermodynamic fluctuation approach is not viable for a most general non-perturbatively completed QCD in the framework of non-equilibrium statistical mechanics with an infinite extensive environment, which we would like to investigate in the near future. The basic idea involved here is that the positivity of the thermodynamic metric tensor cannot be ensured for the full range of all parameters $\{\mu_i, T, V, S\}$, which is necessary for a local minimum of the energy for any given equilibrium configuration. Thus, it is plausible to investigate such notions in a restricted fashion where fluctuations of one or more thermodynamic parameter is either frozen out or assumed to be negligible, see for example [27] in the context of QCD.

B. Hot QCD near T_C

In this paper, we have introduced such geometries to the thermodynamics of hot QCD, and focused our attention on the intrinsic Riemannian geometry in the neighborhood of $T_C(\mu_1, \mu_2)$ of the 2-flavor, as well as of the 3-flavor hot QCD. The geometry thus defined on a two dimensional manifold is solely spanned by the chemical potentials of quasi-particles and in turn determines the two point correlation functions and an associated correlation volume, near the considered transition temperature of the underlying microscopic theory. Note further that all

those QCD-diagrams which just have one gluon exchange do not appear in the thermodynamic geometry, which is due to the fact that such diagrams vanish under color neutrality transformations. Whereas, the corresponding diagrams with two gluon exchange remain non-zero, because the fermion loops are even functions of the chemical potentials and thus contribute to the off-diagonal susceptibility tensors only at zero chemical potentials. We thus find that components of the off-diagonal susceptibility tensor macroscopically correspond to those of the thermodynamic metric tensor $\{g_{ij}|i \neq j\}$, which may further be envisaged in terms of the fermion number density as $g_{ij} \equiv \chi_{ij} = \frac{\partial \mathcal{N}_i}{\partial \mu_j}$. Our geometric study thus describes the mixing between different flavors induced by the resummation of quark loops along the soft, internal, gluon lines to certain orders of given QCD diagrams.

1. 2-flavor Hot QCD

It is worth to point out in the case of 2-flavor QCD that the components of the diagonal quark susceptibility tensor and those of the off-diagonal quark susceptibility tensor may easily be read off just from the components of the associated thermodynamic metric tensors at zero quark chemical potentials. In particular, we see that the diagonal quark susceptibility tensor components g_{μ_i, μ_i} take identical values, while those of the off-diagonal quark susceptibility tensor identically vanish. It is straightforward to see that the determinant of the metric tensor at zero chemical potentials takes a positive definite value and thus defines a well-defined thermodynamic geometry, while the associated scalar curvature at this value of the chemical potentials turns out to be zero, and thus the underlying statistical system at this point becomes a non-interacting system. It turns out that both the diagonal and off-diagonal quark susceptibility tensors, the determinant and the scalar curvature of such associated metric tensor at zero chemical potentials remain intact under the $(\frac{\mu}{T})^4$ -contributions.

It is worth to note that the geometrical results of QCD, when plotted in a physically interesting, near T_C^0 , range against the chemical potentials are in turn very illuminating. In particular, for the case of 2-flavor QCD we find that there are two distinct curves of bumps of varying strength of thermodynamical interactions, whose size thus depends on the chosen domain in the chemical potential space of the system. Furthermore, the determinant of the metric tensor, when plotted against the chemical potentials in the considered domains of hot QCD, has been observed to be a regular increasing function of the chemical potentials. Interestingly, the conclusions to be drawn in this range of the chemical potentials remain the same under the $(\frac{\mu}{T})^4$ -contributions and it turns out that the shape of the determinant of the metric tensor against the chemical potentials remains exactly the same as that without such contributions. However, the curves of the interactions present get aligned with an enhanced

magnitude compared to that without $(\frac{\mu}{T})^4$ -contributions for 2-flavor hot QCD. It is further important to note that the determinant of the metric tensor when plotted against the chemical potentials becomes a smoother function under the thermal contributions. Under the latter the domain of the interactions is observed to be shifted towards the origin, and in particular they are dominant in the range when both chemical potentials lie within $0.1 < \mu_i < 0.2$.

2. 3-flavor Hot QCD

In this case, we observe the same for the case of 3-flavor QCD, i.e. that at zero chemical potentials the components of the metric tensor g_{μ_i, μ_i} reduce to identical values and in fact vanish corresponding to the case of g_{μ_1, μ_2} , which thus respectively describe the diagonal and the off-diagonal quark susceptibility tensors. Moreover, we find that the determinant of the metric tensor acquires a non-zero positive definite value, while the associate scalar curvature turns out again to be zero, and thus the underlying QCD system turns out to be a non-interacting statistical system at zero quarks chemical potentials. It is important to note in this case that the diagonal quark susceptibility tensor components at zero chemical potentials do not find the same values under the $(\frac{\mu}{T})^4$ -contributions but rather we observe $g_{\mu_1, \mu_1} = 0.61$, $g_{\mu_2, \mu_2} = 0.22$ and $g_{\mu_1, \mu_2} = 0$. This further implies that the associated quark susceptibility matrix is non-trivial, and thus the different quarks acquire non-identical two point correlation functions near T_C . However, the determinant of the metric tensor or the geometric invariant objects such as the scalar curvature at zero quarks chemical potentials indeed remain the same under $(\frac{\mu}{T})^4$ -contributions.

In contrast to the 2-flavor QCD, the case of 3-flavor QCD shows that the determinant of the metric tensor, when plotted against the chemical potentials, has two lines of the minima, and the corresponding maximum exactly occurs when either one of the chemical potential reaches the maximum, while the other is held fixed at the origin. In this case, it is observed that there are just two distinct bumps of the thermodynamical interactions of varying heights, instead of the two curves of 2-flavor QCD. Since such thermodynamical interactions are local in nature, thus the height of the observed bumps depend on the domain chosen in the underlying space of chemical potential which characterizes our QCD system. We however find in the 3-flavor hot QCD that the shape of the determinant of the metric tensor appears flatter, and that the number of bumps is increased under $(\frac{\mu}{T})^4$ -contributions, which in fact indicates that the underlying configuration characterized as an internal manifold of the chemical potentials is a strongly interacting statistical system. It turns out that the determi-

nant of the metric tensor, with the inclusion of thermal fluctuations, acquires two finite size bumps when plotted against the chemical potentials. In particular, we observe that there are two bumps of interactions present when either one of the chemical potentials reaches $\mu_i = 0.1$, whereas such bumps do not appear in the determinant of the metric tensor in this range of chemical potentials. It may further be observed that the strength of the local thermal interactions becomes diverse with the amplitude of $10^2 GeV^4$ to $10^4 GeV^4$ of the interactions near the $(\mu_1, \mu_2) = (0.1, 0.1) GeV$.

C. Perspective Features

We have thus provided a very general account of hot QCD thermodynamic geometries and systematically explored the underlying thermodynamic space as an intrinsic Riemannian manifold, and in particular, introduced a covariant geometric notion for both the case of 2-flavor and 3-flavor QCD in the realism of quasi-particle theories with two distinct chemical potentials. In both the case of the 2- and 3-flavor hot QCDs, we find that the domain of the thermodynamical interaction gets shifted towards the origin under the local thermal contributions. The geometric construction as a covariant intrinsic Riemannian manifold provides prominent realization of the limiting equilibrium thermodynamics of the hot QCD near T_C . The present investigation offers an intrinsic geometric exercise of the quasi-particle models of QCD, which have been described by the quark chemical potentials with a transition temperature and thus exhibit convincing macroscopic versus microscopic duality relations via the fermion number density, as the mixing between different flavors/colors encoded in the corresponding partition function of effective gauge field theory.

In summary, we have presented a covariant intrinsic Riemannian geometric perspective of any given analytically calculable quark number susceptibility tensor, which appears naturally within an approximately self-consistent resummation of perturbative QCD. It is worth to mention that the investigations thus demonstrated are however perturbative in nature, but the same line of thought may further be applied for the geometric realization of the underlying quark susceptibility tensors either in the fabric of lattice QCD or that of non-perturbative QCD, see for example [2]. In particular, it will be interesting to see whether this kind of approach can be pushed further, for example to predict geometric properties of chemical correlations, under sizeable higher order perturbative QCD contributions, as well as in general to ascertain geometric features to explore the complete non-perturbative QCD.

Acknowledgments:

VC and BNT acknowledge “C.S.I.R-New Delhi, India” for the financial support.

-
- [1] J.-P. Blaizot, E. Iancu, A. Rebhan, Phys. Lett. **B523**, 143 (2001) [arXiv:hep-ph/0110369v3](#).
- [2] R. V. Gavai, S. Gupta, P. Majumdar, [hep-lat/0110032](#) (2001).
- [3] K. Huang: Statistical Mechanics, John Wiley, 1963, L. D. Landau, E. M. Lifshitz: Statistical Physics-I,II Pergamon, 1969.
- [4] F. Weinhold, J.Chem. Phys. **63**, 2479 (1975), *ibid* J. Chem. Phys **63**, 2484 (1975).
- [5] G. Ruppeiner, Rev. Mod. Phys **67** 605 (1995), Erratum **68**,313 (1996); M. Santoro, A. S. Benight, [math-ph/0507026](#) .
- [6] G. Ruppeiner, Phys. Rev. **A 20**, 1608 (1979); Phys. Rev. Lett **50**, 287 (1983); Phys. Rev. **A 27**, 1116 (1983); G. Ruppeiner, C. Davis, Phys. Rev. **A 41**, 2200 (1990).
- [7] B. N. Tiwari, [arXiv:0801.4087v1 \[hep-th\]](#); T. Sarkar, G. Sengupta, B. N. Tiwari, JHEP **10**, 076 (2008)[arXiv:0806.3513v1 \[hep-th\]](#); S. Bellucci, B. N. Tiwari; [arXiv:0808.3921v1 \[hep-th\]](#).
- [8] S. Bellucci, S. Ferrara, A. Marrani, [arXiv:hep-th/0702019](#). S. Bellucci, S. Ferrara, A. Marrani, [arXiv:0805.1310](#).
- [9] G. Ruppeiner, Phys. Rev. **D 75**, 024037 (2007).
- [10] S. Ferrara, G. W. Gibbons, R. Kallosh, Nucl. Phys. **B500**, 75 (1997) [hep-th 9702103](#).
- [11] J. Y. Shen, R. G. Cai, B. Wang, R. K. Su, [gr-qc/0512035](#).
- [12] J. E. Aman, I. Bengtsson, N. Pidokrajt, [gr-qc/0601119](#); Gen. Rel. Grav. **35**, 1733 (2003) [gr-qc/0304015](#); J. E. Aman, N. Pidokrajt, Phys. Rev. **D73**, 024017 (2006) [hep-th/0510139](#); G. Arcioni, E. Lozano-Tellechea, Phys. Rev. **D 72**, 104021 (2005) [hep-th/ 0412118](#).
- [13] J. P. Blaizot, E. Iancu, [hep-ph/0101103](#) (2001).
- [14] A. Rebhan, [hep-ph/0105183](#) (2001).
- [15] Juan M. Maldacena: Adv. Theor. Math. Phys. **2** (1998) 231-252; Int. J. Theor. Phys. **38**, 1113 (1999) [arXiv:hep-th/9711200v3](#)
S. Bellucci, E. Ivanov, S. Krivonos, Phys. Rev. **D 66**, 086001 (2002); Erratum-ibid. **D 67**,049901 (2003) [arXiv:hep-th/0206126](#).
- [16] J. P. Blaizot, E. Iancu, A. Rebhan, Phys. Rev. **D 63**, 065003 (2001).
- [17] T. Sarkar, G. Sengupta, B. N. Tiwari, JHEP **0611**, 015 (2006) [arXiv:hep-th/0606084](#).
- [18] Cheng *et. al.*, [arXiv:0710.0354](#).
- [19] Frithjof Karsch, Nucl. Phys. **A698**, 199 (2002) [arXiv:hep-ph/0103314](#).
- [20] Boyd *et al.*, Nucl. Phys. **B 469**, 419 (1996) [hep-lat/9602007](#).
- [21] R. Baier, K. Redlich, Phys. Rev. Lett. **84**, 2100 (2000) [arXiv:hep-ph/9908372](#).
- [22] K. Kajantie, M. Laine, K. Rummukainen, Y. Schroder, Phys. Rev. **D 67**, 105008 (2003), [arXiv:hep-ph/0211321](#).
- [23] Vinod Chandra, Ravindra Kumar and V. Ravishankar, Phys. Rev. **C 76**, 054909 (2007); Vinod Chandra, V. Ravishankar, [arXiv:0805.4820](#)(To appear in EPJC); [arXiv:0812.1430](#); V. Chandra, A. Ranjan and V. Ravishankar, [arXiv:0801.1286](#).
- [24] A. Vuorinen, Phys. Rev. **D 68**, 054017 (2003).
- [25] C. R. Allton, S. Ejiri, S. J. Hands, O. Kaczmarek, F. Karsch, E. Laermann, C. Schmidt, L. Scorzato, Phys. Rev. **D 66**, 074507 (2002); F. Karsch, C. R. Allton, S. Ejiri, S. J. Hands, O. Kaczmarek, E. Laermann, C. Schmidt, L. Scorzato, Nucl. Phys. Proc. Suppl. **129**, 614 (2004), [hep-lat/0309116](#).
- [26] O. Kazmarek and F. Zantow, POS (LAT-2005) 177.
- [27] A. Tawfik, J. Phys. G: Nucl. Phys. **31**, S1105 (2005).